

THE REDSHIFT AND THE ORDINARY HOST GALAXY OF GRB 970228¹

J. S. BLOOM, S. G. DJORGOVSKI, S. R. KULKARNI

Palomar Observatory 105–24, California Institute of Technology, Pasadena, CA 91125, USA;
jsb,george,srk@astro.caltech.edu

Submitted to The Astrophysical Journal

ABSTRACT

The gamma-ray burst of 28 February 1997 (GRB 970228) ushered in the discovery of the afterglow phenomenon. Despite intense study of the host galaxy, however, the nature of the host and the distance to the burst eluded the community. Here we present the measurement of the redshift of GRB 970228, and, based on its spectroscopic and photometric properties, identify the host as an underluminous, but otherwise normal galaxy at redshift $z = 0.695$ undergoing a modest level of star formation. At this redshift, the GRB released an isotropic equivalent energy of $E = (6.8 \pm 0.5) \times 10^{51} h_{65}^{-2}$ erg [30–2000 keV restframe]. We find no evidence that the host is much bluer or forming stars more rigorously than the general field population. In fact, by all accounts in our analysis (color–magnitude, magnitude–radius, star-formation rate, Balmer-break amplitude) the host properties appear typical for faint blue field galaxies at comparable redshifts.

Subject headings: cosmology: miscellaneous — cosmology: observations — gamma rays: bursts

1. INTRODUCTION

The gamma-ray burst of 28 February 1997 (hereafter GRB 970228) was a watershed event, especially at optical wavelengths. The afterglow phenomenon, long-lived multiwavelength emission, was discovered following GRB 970228 in the X-rays (Costa *et al.* 1997) and optical (van Paradijs *et al.* 1997). Despite intense observations, no radio transient of GRB 970228 was found (Frail *et al.* 1998); the first radio afterglow (Frail *et al.* 1997) had to await the next BeppoSAX localization of GRB 970508. The basic predictions of the synchrotron shock model for GRB afterglow appeared confirmed by GRB 970228 (*e.g.*, Wijers, Rees & Mészáros 1997).

Despite intense efforts, early spectroscopy of the afterglow GRB 970228 (*e.g.*, Tonry *et al.* 1997, Kulkarni *et al.* 1997) failed to reveal the redshift. Spectroscopy of the afterglow of GRB 970508 proved more successful (Metzger *et al.* 1997), revealing that GRB originated from a redshift $z \gtrsim 0.835$. Through the preponderance of redshift determinations and the association of GRBs with faint galaxies, it is now widely believed that the majority or all of long duration ($T \gtrsim 1$ s) gamma-ray bursts originate from cosmological distances.

Even without a redshift, observations of the afterglow of GRB 970228 in relation to its immediate environment began to shed light on the nature of the progenitors of gamma-ray bursts. Groundbased observations of the afterglow revealed a near coincidence of the GRB with the optical light of a faint galaxy (Metzger *et al.* 1997, van Paradijs *et al.* 1997). Later, deeper groundbased images (Djorgovski *et al.* 1997) and high resolution images from the *Hubble Space Telescope* (HST) showed the light from the fading transient clearly embedded in a faint galaxy (Sahu *et al.* 1997), the putative host of the GRB. Further, these HST images showed a measurable offset between the host galaxy centroid and the afterglow. Though by no

means definitive, the offset of GRB 970228 rendered an active galactic nucleus (AGN) origin unlikely (Sahu *et al.* 1997).

The two most popular progenitor scenarios—coalescence of binary compact stellar remnants and the explosion of a massive star (“collapsar”)—imply that the gamma-ray burst rate should closely follow the massive star formation rate in the Universe. In both formation scenarios a black hole is created as a byproduct; however, the scenarios differ in two important respects. First, only very massive progenitors ($M_{\text{ZAMS}} \gtrsim 40 M_{\odot}$; Fryer, Woosley, & Hartmann 1999) will produce GRBs in the single star model whereas the progenitors of neutron star–neutron star binaries need only originate with $M_{\text{ZAMS}} \gtrsim 8 M_{\odot}$. Second, the scenarios predict a distinct distribution of physical offsets (*e.g.*, Paczyński 1998, Bloom, Sigurdsson & Pols 1999) in that the coalescence site of merging remnants could occur far from the binary birthplace (owing to substantial systemic velocities acquired during neutron star formation through supernovae) whereas exploding massive stars will naturally occur in star-forming regions. In relation to the predicted offset of GRB 970228, Bloom *et al.* (1999) further noted the importance of redshift to determine the luminosity (and infer mass) of the host galaxy: massive galaxies more readily retain binary remnant progenitors. Thus the relationship of GRBs to their hosts is most effectively exploited with redshift by setting the physical scale of any observed angular offset and critically constraining the mass (as proxied by host luminosity).

The redshift of GRB 970228 also plays a critical role in the emerging supernova–GRB link. Following the report of an apparent supernova component in the afterglow of GRB 980326 (Bloom *et al.* 1999), the afterglow light curves of GRB 970228 were reanalyzed: both Reichart (1999) and Galama *et al.* (2000) found evidence for a supernova component. This interpretation, however, relies critically on

¹Partially based on the observations obtained at the W. M. Keck Observatory which is operated by the California Association for Research in Astronomy, a scientific partnership among California Institute of Technology, the University of California and the National Aeronautics and Space Administration.

the knowledge of the redshift to GRB 970228 to set the restframe wavelength of the apparent broadband break of the SN component.

Finally, knowledge of redshift is essential to derive the physical parameters of the GRB itself, primarily the energy scale. We now know, for instance, that the typical GRB releases about 10^{52} erg in gamma-rays. The distribution of observed isotropic-equivalent GRB energies is, however, very broad (*cf.* Kulkarni et al. 2000).

Recognizing these needs we implemented an aggressive spectroscopy campaign on the host of GRB 970228 as detailed in §2. The redshift determination was first reported by Djorgovski et al. (1999) and is described in more detail in §3. We then use this redshift and the spectrum of the host galaxy in §4 to set the physical scale of the observables: energetics, star-formation rates, and offsets. Based on this and photometric imaging from HST we demonstrate in §5 that the host is an underluminous, but otherwise normal galaxy. Lastly, we compare the host with that of the field galaxy population.

2. OBSERVATIONS AND REDUCTIONS

Spectra of the host galaxy were obtained on the W. M. Keck Observatory 10 m telescope (Keck II) atop Mauna Kea, Hawaii. Observations were conducted over the course of several observing runs: UT 1997 August 13, UT 1997 September 14, UT 1997 November 1 and 28–30, and UT 1998 February 21–24. The observing conditions were variable, from marginal (patchy/thin cirrus or mediocre seeing) to excellent, and on some nights no significant detection of the host was made; such data were excluded from the subsequent analysis. On most nights, multiple exposures (2 to 5) of 1800 sec were obtained, with the object dithered on the spectrograph slit by several arcsec between the exposures. The net total useful on-target exposure was approximately 11 hours from all of the runs combined.

All data were obtained using the *Low-Resolution Imaging Spectrometer* (LRIS; Oke et al. 1995) with 300 lines mm^{-1} grating and a 1.0 arcsec wide long slit, giving an effective instrumental resolution FWHM $\approx 12 \text{ \AA}$. Slit position angle was always set to 87° , with star S1 (van Paradijs et al. 1997) always placed on the slit, and used to determine the spectrum trace along the chip; galaxy spectra were then extracted at a position 2.8 arcsec east of the star S1. Efforts were made to observe the target at hour angles so as to make this slit position angle as close to parallactic as possible. Exposures of an internal flat-field lamp and arc lamps were obtained at comparable telescope pointings immediately following the target observations. Exposures of standard stars from Oke & Gunn (1983) and Massey et al. (1998) were obtained and used to measure the instrument response curve, although on some nights the flux zero points were unreliable due to non-photometric conditions.

Wavelength solutions were obtained from arc lamps in the standard manner, and then a second-order correction was determined from the wavelengths of isolated strong night sky lines, and applied to the wavelength solutions. This procedure largely eliminates systematic errors due to the instrument flexure, and is necessary in order to combine the data obtained during separate nights. The final wavelength calibrations have the r.m.s. $\sim 0.2 - 0.5 \text{ \AA}$, as determined from the scatter of the night sky line centers.

All spectra were then rebinned to a common wavelength scale with a sampling of 2.5 \AA (the original pixel scale is $\sim 2.45 \text{ \AA}$), using a Gaussian with a $\sigma = 2.5 \text{ \AA}$ as the interpolating/weighting function. This is effectively a very conservative smoothing of the spectrum, since the actual instrumental resolution corresponds to $\sigma \approx 5 \text{ \AA}$.

Individual spectra were extracted and combined using a statistical weighting based on the signal-to-noise ratio determined from the data themselves (rather than by the exposure time). Since some of the spectra were obtained in non-photometric conditions, the final spectrum flux zero-point calibration is also unreliable, but the spectrum shape should be unaffected. We use direct photometry of the galaxy to correct this zero-point error (see below).

Our uncorrected spectrum gives a spectroscopic magnitude $V \approx 26.3$ mag for the galaxy. Direct photometry from the HST data indicates $V = 25.75 \pm 0.3$ (Galama et al. 2000). Given that some of our spectra were obtained through thin cirrus, this discrepancy is not surprising. Thus, in order to bring our measurements to a consistent system, we multiply our flux values by a constant factor of 1.66, but we thus also inherit the systematic zero-point error of $\sim 30\%$ from the HST photometry.

There is some uncertainty regarding the value of the foreground extinction in this direction (see discussion in §4.3). We apply a Galactic extinction correction by assuming $E_{B-V} = 0.234$ mag from Schlegel, Finkbeiner & Davis (1998). We assume $R_V = A_V/E_{B-V} = 3.2$, and the Galactic extinction curve from Cardelli, Clayton & Mathis (1988) to correct the spectrum. All fluxes and luminosities quoted below incorporate both the flux zero-point and the Galactic extinction corrections.

3. THE REDSHIFT OF GRB 970228

The final combined spectrum of the galaxy is shown in Figure 1. Two strong emission lines are seen, [O II] 3727 and [O III] 5007, thus confirming the initial redshift interpretation based on the [O II] 3727 line alone (Djorgovski et al. 1999). Unfortunately the instrumental resolution was too coarse to resolve the [O II] 3727 doublet. The weighted mean redshift is $z = 0.6950 \pm 0.0003$. A possible weak emission line of [Ne III] 3869 is also seen. Unfortunately, the strong night sky OH lines preclude the measurements of the H β 4861 and [O III] 4959 lines, as well as the higher Balmer lines.

The corrected [O II] 3727 line flux is $(2.2 \pm 0.1) \times 10^{-17}$ erg $\text{cm}^{-2} \text{ s}^{-1} \text{ Hz}^{-1}$, and its observed equivalent width is $W_\lambda = 51 \pm 4 \text{ \AA}$, *i.e.*, $30 \pm 2.4 \text{ \AA}$ in the restframe. This is not unusual for field galaxies in this redshift range (Hogg et al. 1998). The [Ne III] 3869 line, if real, has a flux of at most 10% of the [O II] 3727 line, which is reasonable for an actively star forming galaxy. The corrected [O III] 5007 line flux is $(1.55 \pm 0.12) \times 10^{-17}$ erg $\text{cm}^{-2} \text{ s}^{-1} \text{ Hz}^{-1}$, and its observed equivalent width is $W_\lambda = 30 \pm 2 \text{ \AA}$, *i.e.*, $17.7 \pm 1.2 \text{ \AA}$ in the restframe. For the H β line, we derive an upper limit of $< 3.4 \times 10^{-18}$ erg $\text{cm}^{-2} \text{ s}^{-1} \text{ Hz}^{-1}$ ($\sim 1 \sigma$), and for its observed equivalent width $W_\lambda < 7 \text{ \AA}$. We note however that this measurement may be severely affected by the poor night sky subtraction.

The continuum flux at $\lambda_{obs} = 4746 \text{ \AA}$, corresponding to $\lambda_{rest} = 2800 \text{ \AA}$, is $F_\nu = 0.29 \mu\text{Jy}$, with our measurement uncertain by $\sim 10\%$. The continuum flux at

$\lambda_{obs} \sim 7525 \text{ \AA}$, corresponding to the restframe B band, is $F_\nu = 0.77 \mu\text{Jy}$, with our measurement uncertain by $\sim 7\%$. Above, we report only the statistical uncertainties of all fluxes; an additional systematic uncertainty of $\sim 30\%$ is inherited from the overall flux zero-point uncertainty.

4. IMPLICATIONS OF THE REDSHIFT

For the following discussion, we will assume a flat cosmology as suggested by recent results (*e.g.*, de Bernardis *et al.* 2000) with $H_0 = 65 \text{ km s}^{-1} \text{ Mpc}^{-1}$, $\Omega_M = 0.3$, and $\Lambda_0 = 0.7$. For $z = 0.695$, the luminosity distance is $1.40 \times 10^{28} \text{ cm}$, and 1 arcsec corresponds to 7.65 proper kpc or 13.0 comoving kpc in projection.

4.1. Burst Energetics

The gamma-ray fluence (integrated flux over time) is converted from count rates under the assumption of a GRB spectrum, the spectral evolution, and the true duration of the GRB. These quantities are estimated from the GRB data itself but can lead to large uncertainties (a factor of few) in the fluence determination. In table 1 we summarize the fluence of GRB 970228 as observed by all high energy experiments that detected the GRB. We determine the implied energy release (col. 5, table 1) assuming isotropic emission. Further we “standardize” the energetics to the restframe 30–2000 keV in the following manner. We first normalize the observed fluences in a given bandpass (col. 2 and 3) to a bandpass defined by $30/(1+z)$ to $2000/(1+z)$ keV by a ratio of the integrated spectral shape over these two bandpasses. The implied energy release is then found assuming isotropic emission and using the luminosity distance measure for the assumed cosmology. If no spectral fit is reported we find the median energy implied by assuming the spectral shape is each of the average 54 spectra from Band *et al.* (1993). The reported errors reflect the uncertainty in the redshift measure, fluence, and spectral shape.

Given the significantly higher gamma-ray spectral and timing resolution of the TGRS instrument relative to the others, we favor the isotropic energy implied by the TGRS analysis: $E = (6.8 \pm 0.5) \times 10^{51} h_{65}^{-2} \text{ erg}$ [30–2000 keV restframe]. That the implied energy is a factor of ~ 2 –3 higher using measurements from BeppoSAX and Ulysses reflects the importance of high signal-to-noise spectroscopy in ascertaining the fluence and hence the energy release. The slow decline and absence of a strong break in the optical light curve (*e.g.*, Galama *et al.* 1997) suggests that the GRB emission was nearly isotropic (see also Sari, Piran & Halpern 1999) and so the knowledge of E is primarily limited by the accuracy of the fluence measurement.

4.2. The offset of the GRB and the host morphology

For the purpose determining the position of the GRB within its host, we examined the HST/STIS observations taken on 4.7 Sept 1997 UT (Fruchter *et al.* 1999). The observation consisted of eight 575 s STIS clear (CCD50) exposures paired in to four 1150 s to facilitate removal of cosmic rays. We processed these images using the drizzle technique of Fruchter & Hook (1997) to create a final image with a plate scale of $0.0254 \text{ arcsec pixel}^{-1}$. To enhance the low-surface brightness host galaxy we smoothed

this image with a Gaussian with $\sigma = 0.043 \text{ arcsec}$. The optical transient is well-detected in figure 2 (point source towards the South) and clearly offset from the bulk of the detectable emission of the host.

Two morphological features of the host stand out: a bright knot manifested as an sharp $6\text{-}\sigma$ peak near the centroid of the host to north of the transient and an extension from this knot towards the transient. Although, as we demonstrate below, this host is a subluminescent galaxy (*i.e.*, not a classic late-type L_* spiral galaxy) we attribute these features to a nucleus and a spiral-arm, respectively. It is not unusual for dwarf galaxies to exhibit these canonical Hubble-diagram structures (S. Odewahn, private communication). These feature have not previously been noted in the literature.

Centroiding the transient and the nucleus components within a 3 pixel aperture radius about their respective peak, we find an angular offset of $436 \pm 14 \text{ milliarcsec}$ between the nucleus and the optical transient. With our assumed cosmology, this amounts to a projected physical distance of $3.34 \pm 0.11 h_{65}^{-1} \text{ kpc}$.

4.3. Physical Parameters of the host galaxy

We found half-light radius of the host galaxy using our final drizzled HST/STIS image: we mask a 3×3 pixel region around the position of the optical transient and inspect the curve-of-growth centered on the central bright knot, the supposed nucleus and estimate the half-light radius to be 0.31 arcsec or $2.4 h_{65}^{-1} \text{ kpc}$ (physical) at a redshift of $z = 0.695$. The half-light radius visually estimated from curve-of-growth in the WFPC F814W and F606W filters (see Castander & Lamb 1999) is comparable.

Although there is some debate (at the 0.3 mag level in A_V) as to the proper level of Galactic extinction toward GRB 970228 (Castander & Lamb 1999, González, Fruchter & Dirsch 1999, Fruchter *et al.* 1999) we have chosen to adopt the value $E(B - V) = 0.234$ found from the dust maps of Schlegel, Finkbeiner & Davis 1998 and a Galactic reddening curve $R_V = A_V/E(B - V) = 3.2$. Using extensive reanalysis of the *HST* imaging data by Galama *et al.* 2000 the extinction corrected broadband colors of the host galaxy as $V = 25.0 \pm 0.2$, $R_c = 24.6 \pm 0.2$, $I_c = 24.2 \pm 0.2$. These measures, consistent with those of Castander & Lamb (1999) and Fruchter *et al.* (1999), are derived from the WFPC2 colors and broadband STIS flux. The errors reflect both the statistical error and the uncertainty in the spectral energy distribution of the host galaxy. We have not included a contribution from the uncertainty in the Galactic extinction. Using the NICMOS measurement from Fruchter *et al.* (1999) the extinction corrected infrared magnitude is $H_{AB} = 24.6 \pm 0.1$. Using the zero-points from Fukugita *et al.* (1996), the extinction-corrected AB-magnitudes of the host galaxy are: $V_{AB} = 25.0$, $R_{AB} = 24.8$, $I_{AB} = 24.7$.

To facilitate comparison with moderate redshift galaxy surveys (§5) we compute the restframe B -band magnitude of the host galaxy. From the observed continuum in the restframe B band, we derive the absolute magnitude $M_B = -18.4 \pm 0.4 \text{ mag}$ [or $M_{AB}(B) = -18.6 \pm 0.4 \text{ mag}$], *i.e.*, only slightly brighter than the LMC now. For our chosen value of H_0 , an L_* galaxy at $z \sim 0$ has $M_B \approx -20.9 \text{ mag}$, and thus the host at the observed epoch has $L \sim$

0.1 L_* today. Its observed morphology from the HST images is also consistent with a dwarf, low-surface brightness galaxy.

4.4. Star formation in the host

From the [O II] 3727 line flux, we derive the line luminosity $L_{3727} = 5.44 \times 10^{40}$ erg s $^{-1}$ ($\pm 5\%$ random) ($\pm 30\%$ systematic). Using the star formation rate estimator from Kennicutt 1998, we derive the SFR $\approx 0.76 M_\odot$ yr $^{-1}$. Using a 3- σ limit on the H β flux, we estimate $L_{H\beta} < 2.5 \times 10^{40}$ erg s $^{-1}$. Assuming the H α /H β ratio of 2.85 ± 0.2 for the Case B recombination and a range of excitation temperatures, we can derive a pseudo-H α based estimate of the star formation rate (*cf.* Kennicutt 1998), SFR $< 0.6 M_\odot$ yr $^{-1}$, but we consider this to be less reliable than the [O II] 3727 measurement. From the UV continuum luminosity at $\lambda_{rest} = 2800\text{\AA}$, following Madau, Pozzetti & Dickinson (1998), we derive SFR $\approx 0.54 M_\odot$ yr $^{-1}$.

We note that the net uncertainties for each of these independent SFR estimates are at least 50%, and the overall agreement is encouraging. While we do not know the effective extinction corrections in the host galaxy itself, these are likely to be modest, given its blue colors (*cf.* §5), and are unlikely to change our results by more than a factor of two. (We hasten to point out that we are completely insensitive to any fully obscured star formation component, if any is present.) On the whole, the galaxy appears to have a rather modest (unobscured) star formation rate, $\sim 0.5 - 1 M_\odot$ yr $^{-1}$. Given the relatively normal equivalent width of the [O II] 3727 line, even the star formation per unit mass does not seem to be extraordinarily high.

5. THE NATURE OF THE HOST GALAXY

At $M_{AB}(B) = -18.6$, the host galaxy of GRB 970228 is a sub-luminous galaxy roughly 2.7 mag below L_* at comparable redshifts (Lilly *et al.* 1995). Galama *et al.* (2000), based on the redshift of GRB 970228, recently found that an Sc galaxy spectral energy distribution reasonably fits the optical-IR photometric fluxes of the host galaxy. This differs from the analysis of Castander & Lamb (1999) which would, now given the redshift of $z = 0.695$, favor a classification of an ‘‘Irregular’’ galaxy having undergone burst of star-formation over the past few hundred Myr. Clearly it is difficult to precisely determine the galaxy type without more precise photometry and knowledge of the true Galactic extinction, but our identification of a nucleus and possible arm structure (§4.2) supports the idea that the host is a late-type dwarf. Indeed, the host has similar characteristics to that of the Large Magellanic Cloud. We further note that compared with the Simard *et al.* (1999), the magnitude-size relation of the host galaxy is consistent with that observed for late-type and dwarf-irregular galaxies.

The flat continuum suggests little restframe extinction in this galaxy. We found the isophotal ($H - V$) $_{AB}$ color of galaxies in the Hubble Deep Field North (HDF-N) using the published photometry from Thompson *et al.* (1999) (NICMOS: F160W) and Williams *et al.* (1996) (WFPC4: F606W filter). All WFPC object identifications within 0.3 arcsec of a NICMOS identification are plotted in figure 3 along with the dereddened color of the host galaxy of GRB

970228. Our field selection essentially biases the color-magnitude relation towards redder objects and would serve to accentuate the locus of the field with a blue galaxy. Even with this bias, there is no indication that the host is substantially more blue than field galaxies at comparable magnitudes.

This conclusion—that the host galaxy of GRB 970228 is not exceptionally blue—is at odds with that of Fruchter *et al.* (1999) who have claimed that the host galaxy is unusually blue as compared with typical field galaxies. The difference may be due to the fact that the Fruchter *et al.* (1999) analysis compared the host colors with a significantly more shallow infrared survey than the NICMOS HDF essentially masking the trend for faint galaxies to appear more blue.

Figure 4 shows a section of the median-binned spectrum of the host galaxy. The Balmer break is clearly detected, with an amplitude $\Delta m \approx 0.55$ mag, which is typical for the Balmer break selected population of field galaxies at $z \sim 1$ (K. Adelberger, private communication). For reference we also plot several population synthesis model spectra (Bruzual & Charlot 1993). The top panel shows model spectra for a galaxy with a uniform star formation rate, which may be a reasonable time-averaged approximation for a normal late-type galaxy. The correspondence is reasonably good and does not depend on the model age. The bottom panel shows models with an instantaneous burst of star formation. In order to match the data, we require fine-tuning of the post-burst age to be $\sim 10^8 \times 2^{\pm 1}$ yr. No attempt was made to optimize the fit or to seek best model parameters and the purpose of this comparison is simply illustrative. Clearly, if there was an ongoing or very recent burst of star formation, the spectrum would be much flatter, with a weaker Balmer break.

6. DISCUSSION AND CONCLUSION

We have determined the redshift of the host galaxy of GRB 970228 to be $z = 0.695$ based on [O II] 3727 and [O III] 5007 line emission. The implied energy release $(6.8 \pm 0.5) \times 10^{51}$ [30–2000 keV restframe] is on the smaller end of, but still comparable to, the handful of other bursts with energy determinations (*e.g.*, Kulkarni *et al.* 2000). The absence of a detectable break in the afterglow light curve we take to imply that any collimation of emission (*i.e.*, jetting) negligibly reduces the estimate of total energy release in GRB 970228 (although Frail, Waxman & Kulkarni 2000, using late-time radio data, have found that even without an optical break, GRB 970508 may have been collimated).

Most GRB transients appear spatially coincident with faint host galaxies, disfavoring the merging NS hypothesis (*e.g.*, Paczyński 1998). The coincidence of GRB 970508 with its host (Fruchter & Pian 1998, Bloom *et al.* 1998) is particularly constraining given the excellent spatial coincidence of the GRB with the center of a dwarf galaxy (*cf.* Bloom *et al.* 1998). The transient of GRB 970228 lies $3.34 \pm 0.11 h_{65}^{-1}$ kpc from the center of the galaxy, about 1 kpc in projection outside the half-light radius of the galaxy. From the above analysis we have shown, like GRB 970508, the host is underluminous ($L \approx 0.05 L_*$), and by assumption, undermassive relative to L_* galaxies. According to Bloom *et al.* (1999), about 50% of merging

neutron binaries should occur beyond 3.5 kpc in projection of such dwarf galaxies. Thus, by itself, the offset of GRB 970228 from its host does not particularly favor a progenitor model.

With a star-formation rate of $0.5\text{--}1 M_{\odot} \text{ yr}^{-1}$, the host of GRB 970228 is forming stars only at a moderately higher rate than comparable galaxies in the local universe. This result is not surprising given that, on a whole, the universal rate of star-formation increases steeply at least out until redshift $z \approx 1.5$. If the association of GRBs with massive stars is correct, however, GRB hosts should reveal an increased propensity to form massive stars over and above their counterpart field galaxies. Moreover, the massive star formation rate should be vigorous at the time GRB occurs since massive stars require a negligible time (compared to typical star-formation burst durations) to explode since zero-age main sequence.

In R -band magnitude the host is near the median of GRB hosts observed to date but in absolute B -band magnitude the host at the faint end of the distribution. Of the host galaxies detected thus far only GRB 970508 is as comparably faint to the host of GRB 970228. Except in

angular extent, the host galaxies of GRB 970228 and GRB 970508 (Bloom *et al.* 1998) bear a striking resemblance. Both appear to be sub-luminous ($L \lesssim 0.1L_{*}$), compact and blue. Spectroscopy of both reveal the presence of the [Ne III] 3869 line, indicative of recent very massive star formation. However, such properties are not shared by all of the GRB hosts studied to date. We note too the rather curious trend that the two GRBs themselves appear to have similar properties in that they decay slowly, are the two least luminous in term of GRB energetics, and do not exhibit evidence of a strong break in the light curve.

The authors thank the generous support of the staff of the W. M. Keck Foundation. This paper has benefited from stimulating conversations with P. van Dokkum and K. Adelberger. We thank M. van Kerkwijk for help during observing and C. Clemens for his use of dark-time observing nights. JSB gratefully acknowledges the fellowship from the Fannie and John Hertz Foundation. SGD acknowledges partial funding from the Bressler Foundation. This work was supported in part by grants from the NSF and NASA to SRK.

REFERENCES

- Band, D. *et al.* 1993, ApJ, 413, 281.
 Bloom, J. S., Djorgovski, S. G., Kulkarni, S. R., and Frail, D. A. 1998, ApJ, 507, L25.
 Bloom, J. S., Sigurdsson, S., and Pols, O. R. 1999, MNRAS, 305, 763.
 Bloom, J. S. *et al.* 1999, Nature, 401, 453.
 Bruzual, A. G. and Charlot, S. 1993, ApJ, 405, 538.
 Cardelli, J. A., Clayton, G. C., and Mathis, J. S. 1988, ApJ, 329, L33.
 Castander, F. J. and Lamb, D. Q. 1999, ApJ, 523, 593.
 Costa, E. *et al.* 1997, Nature, 387, 783.
 de Bernardis, P. *et al.* 2000, Nature, 404, 355.
 Djorgovski, S. G., Kulkarni, S. R., Gal, R. R., Odewahn, S. C., and Frail, D. A. 1997, IAU circular 6372.
 Djorgovski, S. G. *et al.* 1999, GCN notice 289.
 Frail, D. A., Kulkarni, S. R., Nicastro, S. R., Feroci, M., and Taylor, G. B. 1997, Nature, 389, 261.
 Frail, D. A., Kulkarni, S. R., Shepherd, D. S., and Waxman, E. 1998, ApJ, 502, L119.
 Frail, D. A., Waxman, E., and Kulkarni, S. R. 2000, ApJ, 537, 191.
 Frontera, F., Costa, E., dal Fiume, D., Feroci, M., Nicastro, L., Orlandini, M., Palazzi, E., and Zavattini, G. 1997, A&AS, 122, 357.
 Frontera, F. *et al.* 1998, ApJ, 493, L67.
 Fruchter, A. and Pian, E. 1998, GCN notice 151.
 Fruchter, A. S. and Hook, R. N. 1997, in Applications of Digital Image Processing XX, Proc. SPIE, Vol. 3164, ed. A. Tescher, SPIE, 120.
 Fruchter, A. S. *et al.* 1999, ApJ, 516, 683.
 Fryer, C. L., Woosley, S. E., and Hartmann, D. H. 1999, ApJ, 526, 152.
 Fukugita, M., Ichikawa, T., Gunn, J. E., Doi, M., Shimasaku, K., and Schneider, D. P. 1996, AJ, 111, 1748.
 Galama, T. *et al.* 1997, Nature, 387, 479.
 Galama, T. J. *et al.* 2000, ApJ, 536, 185.
 González, R. A., Fruchter, A. S., and Dirsch, B. 1999, ApJ, 515, 69.
 Hogg, D. W., Cohen, J. G., Blandford, R., and Pahre, M. A. 1998, ApJ, 504, 622.
 Hurley, K. *et al.* 1997, ApJ, 485, L1.
 Hurley, K. *et al.* 1992, A&AS, 92, 401.
 Jager, R. *et al.* 1997, A&AS, 125, 557.
 Kennicutt, R. C. 1998, Ann. Rev. Astr. Ap., 36, 189.
 Kulkarni, S. R. *et al.* 2000, in To appear in Proc. of the 5th Huntsville Gamma-Ray Burst Symposium, 21 pages, LaTeX.
 Kulkarni, S. R., Djorgovski, S. G., Clemens, J. C., Gal, R. R., Odewahn, S. C., and Frail, D. A. 1997, IAU Circ, 6732.
 Lilly, S. J., Tresse, L., Hammer, F., Crampton, D., and Le Fevre, O. 1995, ApJ, 455, 108.
 Madau, P., Pozzetti, L., and Dickinson, M. 1998, ApJ, 498, 106.
 Massey, P., Strobel, K., Barnes, J. V., and Anderson, E. 1988, ApJ, 328, 315.
 Metzger, M. R., Kulkarni, S. R., Djorgovski, S. G., Gal, R., Steidel, C. C., and Frail, D. A. 1997, IAU circular 6588.
 Oke, J. B. *et al.* 1995, PASP, 107, 375.
 Oke, J. B. and Gunn, J. E. 1983, ApJ, 266, 713.
 Paczyński, B. 1998, ApJ, 494, L45.
 Palmer, D. M. *et al.* 1998, in Gamma-Ray Bursts, 304.
 Reichart, D. E. 1999, ApJ, 521, L111.
 Sahu, K. C. *et al.* 1997, Nature, 387, 476.
 Sari, R., Piran, T., and Halpern, J. P. 1999, ApJ, 519, L17.
 Schlegel, D. J., Finkbeiner, D. P., and Davis, M. 1998, ApJ, 500, 525.
 Seifert, H. *et al.* 1996, A&AS, 120, C653.
 Simard, L. *et al.* 1999, ApJ, 519, 563.
 Thompson, R. I., Storrie-Lombardi, L. J., Weymann, R. J., Rieke, M. J., Schneider, G., Stobie, E., and Lytle, D. 1999, AJ, 117, 17.
 Tonry, J. L., Hu, E. M., Cowie, L. L., and McMahon, R. G. 1997, IAU circular 6620.
 van Paradijs, J. *et al.* 1997, Nature, 386, 686.
 Wijers, R. A. M. J., Rees, M. J., and Mészáros, P. 1997, MNRAS, 288, L51.
 Williams, R. E. *et al.* 1996, AJ, 112, 1335.

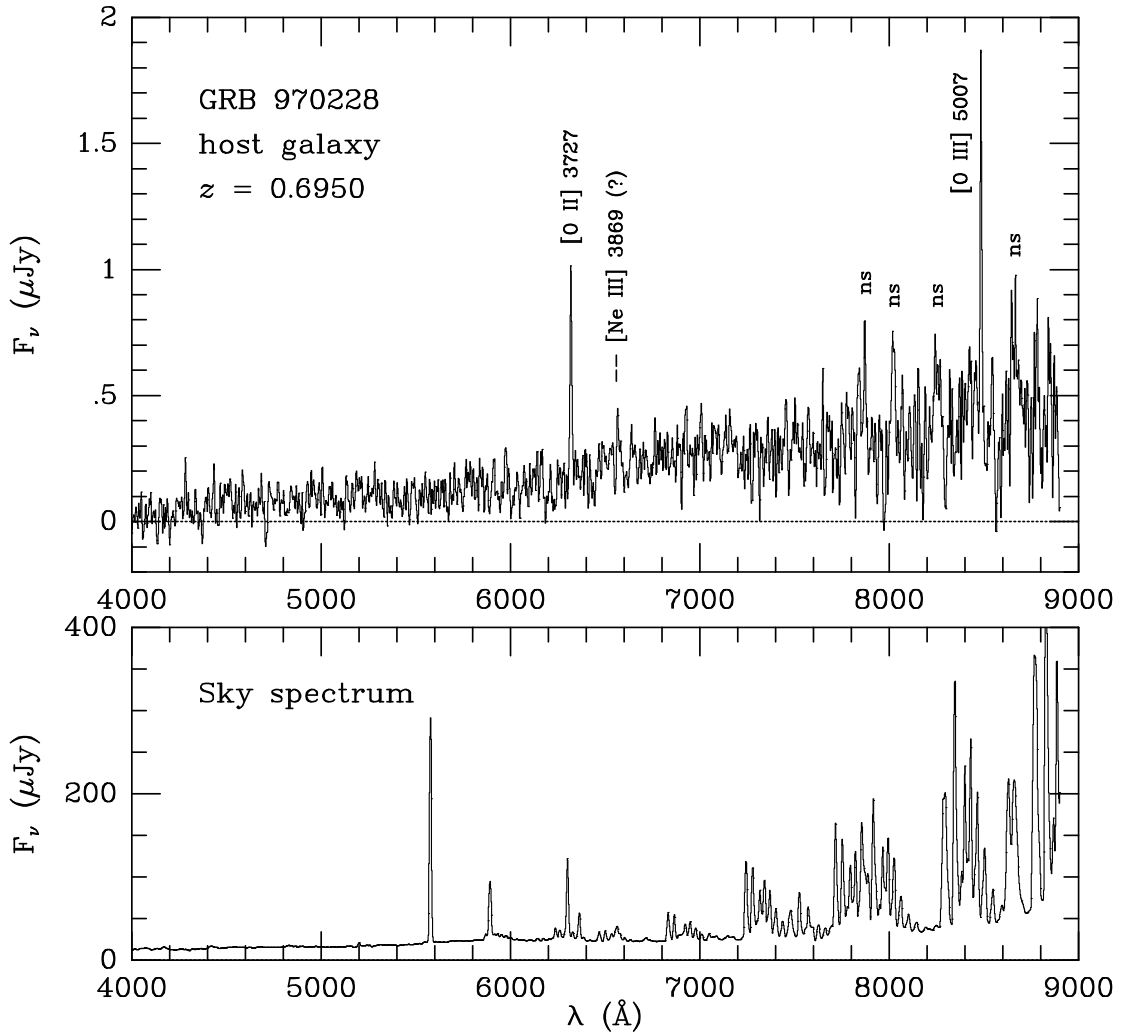


FIG. 1.— (top) The weighted average spectrum of the host galaxy of GRB 970228, obtained at the Keck II telescope. Prominent emission lines [O II] 3727 and [O III] 5007 and possibly [Ne III] 3869 are labeled assuming the lines originate from the host at redshift $z = 0.695$. The notation “ns” refers to noise spikes from strong night sky lines. (bottom) The average night sky spectrum observed during the GRB 970228 host observations, extracted and averaged in exactly the same way as the host galaxy spectrum.

TABLE 1
IMPLIED ENERGETICS OF GRB 970228

Instrument	Bandpass [keV]	S_{-6}^a [erg cm $^{-2}$]	$E_{30-2000}^b$ [$\times 10^{51}$ erg]	Refs.
TGRS/WIND	50–300	3.1 ± 0.2	6.8 ± 0.5	1,2
GRBM+WFC	40–700	11 ± 1	21 ± 2	3,4,5
/BeppoSAX	50–300	6.1	20 ± 6	
GRB/Ulysses	25–100	4.3	31 ± 16	6, 7

REFERENCES— 1. Seifert *et al.* 1996 2. Palmer *et al.* 1998 3. Frontera *et al.* 1997 4. Jager *et al.* 1997 5. Frontera *et al.* 1998 6. Hurley *et al.* 1992 7. Hurley *et al.* 1997

^a Fluence ($\times 10^6$) in given bandpass over the duration of the GRB as determined from spectral fits.

^b Implied energy release in GRB 970228 in the bandpass 30–2000 keV restframe assuming isotropic emission. We have assumed a cosmology with $H_0 = 65$ km s $^{-1}$ Mpc $^{-1}$, $\Omega_M = 0.3$, and $\Lambda_0 = 0.7$. See text for explanation.

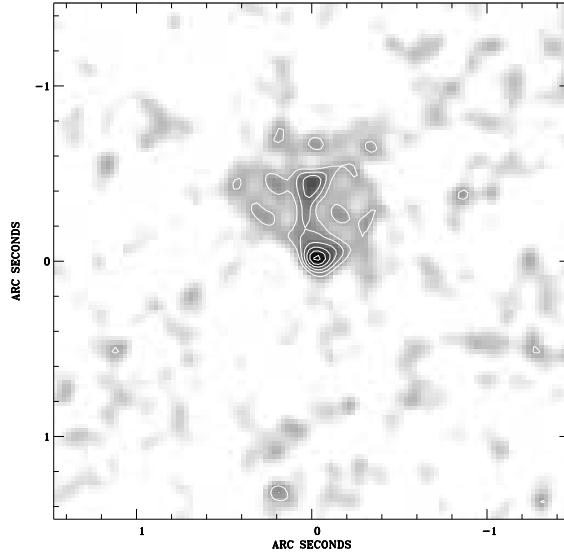


FIG. 2.— A $3'' \times 3''$ (23×23 kpc² in projection) region of the HST/STIS image (4.7 September 1997 UT) of the host galaxy of GRB 970228. The image has been smoothed (see text) and is centered on the optical transient. North is up and East is to the left. Contours in units of 3,4,5,6,7,8 background σ ($\sigma = 2.41$ DN) are overlaid. The transient is found on the outskirts of detectable emission from a faint, low-surface brightness galaxy. The morphology is clearly not that of a classical Hubble type, though there appears to be a nucleus and an extended structure to the north of the transient.

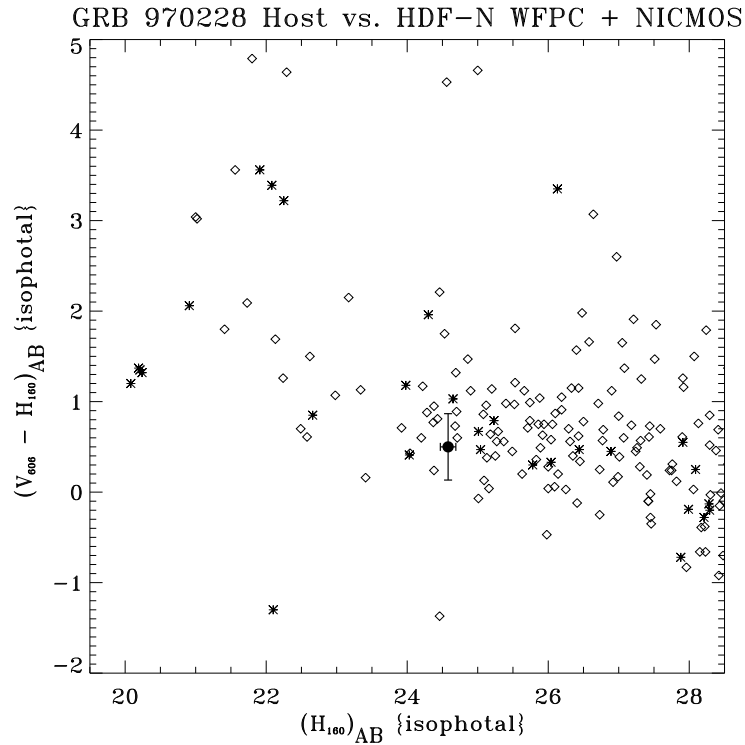


FIG. 3.— Comparison of the color-magnitude of the host galaxy of GRB 970228 with the Hubble Deep Field North (HDF-N). No systematic difference, assuming a Galactic extinction towards GRB 970228 of $A_V = 0.75$, is found between field galaxies at comparable magnitudes and the host (denoted as a solid circle with error bars). NICMOS and WFPC photometry are taken from Thompson *et al.* (1999) and Williams *et al.* (1996), respectively. The diamonds (\diamond) represent extended objects (with the ratio of semi-major to semi-minor axes less than 0.9) and the asterisks (*) compact galaxies and stars. The error bars on the HDF-N data have been suppressed. See the text for an explanation of the selection criteria.

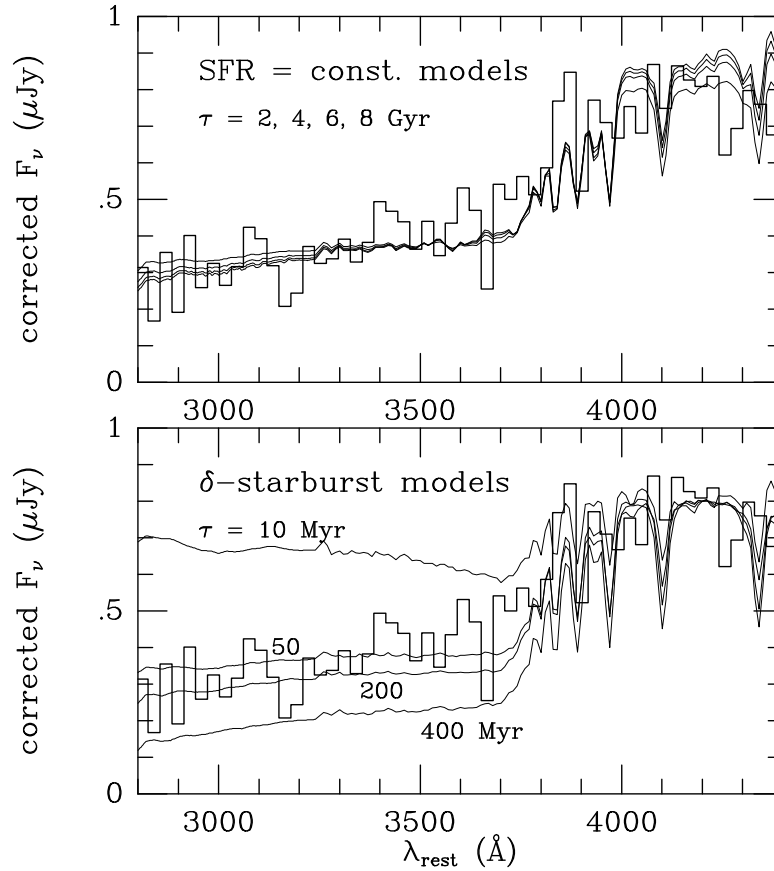


FIG. 4.— Median-binned portion of the host spectrum near the Balmer decrement. (top panel) Overlaid are Bruzual & Charlot (1993) galaxy synthesis models assuming a varying time of constant star formation. (bottom panel) Overlaid are Bruzual & Charlot 1993 galaxy synthesis models assuming an instantaneous burst of star-formation having occurred τ years since observation. Clearly the host continuum could not be dominated by a young population of stars ($\tau = 10$ Myr). See the text for a discussion.